EFFECT OF SPIRAL DESIGN ON CRYSTAL ORIENTATION DURING SINGLE CRYSTAL GROWTH

M. Ghanbari[1], M. R. Aboutalebi[2] and S. G. Shabestari[2]

* *shabestari@iust.ac.ir*

Received: December 2013 **Accepted: March 2014**

[1] School of Metallurgy and Materials Engineering, Iran University of Science and Technology, Iran, Tehran.

[2] Center of Excellence for High Strength Alloys Technology, School of Metallurgy and Materials Engineering, Iran University of Science and Technology, Iran, Tehran.

Abstract: *Geometrical design of the spiral crystal selector can affect crystal orientation in the final single crystal structure. To achieve a better understanding of conditions associated with the onset of crystal orientation in a spiral crystal selector, temperature field was investigated using three-dimensional finite element method during the process. Different geometries of spiral crystal selector were used to produce Al- 3 wt. % Cu alloy single crystal using a Bridgman type furnace. The Crystal orientation of the samples was determined using electron backscattered diffraction (EBSD) and optical microscopy. Analysing the temperature field in the crystal selector revealed that, the orientation of growing dendrites against liquidus isotherm in the spiral selector was the reason for crystal misorientation which differs in various selector geometries. Increasing the take-off angle from 35° up to 45° increases the misorientation with respect to <001> direction. Further increase of take-off angle greater than 45° will decrease the crystal misorientation again and the efficiency of the selector to produce a single grain is decreased.*

Keywords: *spiral crystal selector, crystal orientation, aluminum-copper alloy, EBSD, numerical simulation.*

1. INTRODUCTION

Elimination of high angle grain boundaries and production of single crystal structure is the most effective way to improve the creep resistance of turbine blades for high temperature applications [1, 2]. On the other hand, the formation of <001> texture close to the loading direction is often favourable to improve creep resistance and reduce thermal fatigue. It is as a consequence of lowering the elastic module in metals with FCC crystal structure. [3-5] Therefore, it is interested to produce a single crystal part which consists of a single grain with <001> crystallographic orientation parallel to loading direction.

To develop a grain with <001> crystallographic direction, two methods are employed; first, a seed crystal with a predetermined and favourable orientation can be used as a substrate, and further solidification process can be carried out from the predetermined orientation; and secondly, a spiral crystal selector which is commonly used in industrial applications to produce a single grain. [8] A crystal selector consists of two main components; a starter block which creates a well aligned <001> texture as a result of competitive growth mechanism, [9-11] and a spiral part which select one of the growing grains in the starter block due to blocking of the dendrite stem and branching or widening of secondary dendritic arm mechanism [6, 12-15]. Due to growth anisotropy of cubic metals, <001> crystallographic direction is known as preferred growth direction. As a result of competitive growth mechanism, well aligned dendrites with respect to favourable growth direction will be consistent with less undercooling required for growth. So, if the stems of the dendrites lay parallel or close to the heat flow direction, they would be more consistent. In cubic metals, dendritic arms lay to <001> direction and so, dendrites with stem or secondary arms along the heat flow direction tend to develop easier in comparison with the others. [16]

Single crystal turbine blades are often used with a misorientation of about 15° with respect to the longitudinal axes of the imposed mechanical loads. It is as a result of industrial limitations in the production of spiral crystal selector to produce single crystal piece aligned in the almost <001> direction [6, 7]. The role of crystal

selector in the selection of one grain with a preferred direction is important and many studies are carried out to investigate the effect of spiral design on crystal selection process. [7, 13, 14, 16] Geometrical parameters which determine the execution of a spiral crystal selector are listed as spiral pitch length (Lp), spiral diameter (Ds), the diameter of the spiral channel (dr) and the take-off angle of the spiral part (θ) [13]. Spiral take-off angle (θ) has the greatest effect on the crystal orientation of the final crystal [14]. To improve the production efficiency of SX blades, numerous efforts on the grain selection during SX casting have been made over the last few decades by simulations and experiments [17-19]. Recently, Dai et al.[17] simulated and analyzed the competitive growth and grain selection in the selector with emphasis on the geometric parameters of the specially the spiral take-off angle using a coupled ProCAST and CAFE model. The results showed that the grain selection in spiral become more efficient with the decreasing of the spiral angle. However, the grain orientations cannot be optimized during the selection process in the spiral. It is necessary to get further insight into the relationship between the crystal orientation and the geometries of the spiral grain selector. Furthermore, to enhance the understanding of grain selection and to provide the capability to design and optimize a spiral grain selector for newly developed alloys and components, it is of interest to investigate the mechanism of grain selection in the spiral passage for the attempt to improve the efficiency and reliability of the grain selector. Dai et al. [18] proposed that the geometrical restriction is a dominant factor in the process of grain selection. Gao et al. [19] observed the competitive dendritic growth in spiral passage by experimental methods and verified that the geometrical blocking of narrow passage attributes to the grain selection. Nevertheless, research on the mechanism of grain selection in the spiral should not be limited to the geometrical restriction. It has been established that the competitive growth during directional solidification depends on the relative orientation of grains and their relation with the direction of maximum temperature gradient (the direction of heat flow). In view of the dominant role that the heat flow plays in the competitive grain growth during directional solidification, it is speculated that the heat flow also makes contribution to the grain selection in the spiral passage. However, little attention has been paid to the influence of heat flow on the competitive growth and grain selection in the spiral.

Therefore, this article is devoted to investigate the relationship between the crystal orientations and the geometries of the grain selector. In addition, the influence of heat flow will be taken into account when analyzing the mechanism of grain selection in the spiral passage. The SX casting process is simulated by a coupled ProCAST and CAFE model. In this research the effect of spiral geometry, particularly the effect of spiral take-off angle is investigated on temperature distribution in the spiral channel using finite element ProCAST software. Also, the effect of isotherm direction with respect to the growth direction of dendrites on the final structure of the single crystal is studied. Then, the results are verified experimentally through the single crystal growth of Al-3 wt. % Cu alloy with different spiral geometries in Bridgman type furnace.

2. EXPERIMENTAL PROCEDURE

2. 1. Heat transfer model

The directional solidification process mainly refers to three kinds of heat transfer patterns: the thermal conduction in materials and between different materials that contact each other, the radiation within the insulator and convection heat transfer. In this study, convection heat transfer was ignored. According to the energy conversation, heat transfer in the alloy during the directional solidification process can be formulated as follows:

$$\left(\rho c_p\right)\partial T/\partial t = \nabla\left(k\nabla T\right) - \rho_s L_f \frac{df_s}{dt} + Q \qquad (1)$$

where ρ is the alloy density, c the specific heat capacity, T the temperature, t the time, k the

coefficient of thermal conductivity, L the latent heat and f_s the solid fraction, Q the thermal radiation quantity. Based on the law of Stefen–Boltzman, the thermal radiation quantity, Q can be written as:

$$Q = \sigma\varepsilon(T^4 - T_a^4) \quad (2)$$

Where σ is the Stefan–Boltzmann constant, ε the emissivity, T the surface temperature, and Ta the ambient temperature and namely the inner wall temperature of the furnace.

2. 2. Nucleation Model

The calculated thermal profiles by the macro-scale ProCAST (a trademark of ESI Group, Paris), were then used as input in the meso-scale CAFE model to predict the grain structure with special consideration of the crystallographic anisotropy of grains and the growth kinetics of dendrite tips. In the present study, the heterogeneous nucleation that occurred randomly at the surface of chill plate was modeled by a continuous nucleation distribution called Gaussian distribution of nucleation sites [16]. The continuous nucleation distribution, *dn/ d(ΔT)*, can be described as:

$$\frac{dn}{d(\Delta T)} = \frac{n_{\max}}{\sqrt{2\pi}\Delta T_\sigma}\exp\left[-\frac{1}{2}\left(\frac{\Delta T - \Delta T_{\max}}{\Delta T_\sigma}\right)^2\right] \quad (3)$$

Where *dn* is the grain density increase, which is induced by an increase in the undercooling, *d(ΔT)*. ΔT_{max} is the mean undercooling, ΔT_σ the standard deviation, and n_{max} the maximum density of nuclei obtained by the integral of the Gaussian distribution. The nmax is an important input parameter which is imperative for the CAFE simulation as a nucleation boundary condition. To obtain the value, the grain density at the surface of chill plate was examined quantitatively with EBSD techniques. Under the above experimental condition, the areal density was equal to 1.65×10^8 (number of nuclei/m^2) and this value was used as the nucleation boundary condition, n_{max}, at the chill surface for CAFE simulations.

2. 3. Grain Growth Model

The preferred orientation of Ni-base superalloys with a face-centered cubic crystal structure is <001> crystallographic orientation. It is assumed that the crystallographic orientation of a new nucleus nucleated at the surface of chill plate is random, and the growth directions of the trunks and arms coincide with <001> crystallographic orientation of the parent nucleus. In castings, the dendrite growth is dominated by the undercooling near the dendrite tip. The total undercooling of the dendrite tip, ΔT, is generally the sum of four contributions [31]:

$$\Delta T = \Delta T_C + \Delta T_T + \Delta T_K + \Delta T_R \quad (4)$$

where ΔTC, ΔTT, ΔTK and ΔTR are the undercooling contributions associated with solute diffusion, thermal diffusion, attachment kinetics and curvature, respectively. For most metallic alloys, in the case of directional solidification, the last three contributions that appear in Eq. (4) are small. The growth of the dendrite is primarily controlled by solute diffusion, and the growth kinetics of both columnar and equiaxed morphologies can be calculated with the aid of Kurz–Giovanola–Trivedi (KGT) model [16]. During the process of simulation, the growth rate of dendrite tip was simplified as:

$$v = \alpha_2\Delta T^2 + \alpha_3\Delta T^3 \quad (5)$$

Where α_2 and α_3 are constants, determined by alloy composition according to the KGT model. [20]

Temperature dependent boundary conditions and materials properties were used for numerical simulation. The initial temperature of the molten metal was set to 800°C and a withdrawal rate of 3mm.min^{-1} was applied in all cases. To achieve the equilibrium condition in the process, the mold

was held in the furnace for appropriate soaking time. Simulation results were used to evaluate the conditions of isotherms in the process, particularly at the entrance of the spiral channel.

To investigate the effect of spiral geometry on the misorientation of single crystal during growth process, four different designs of spiral crystal selector have been applied. The main designing parameters including spiral pitch length (L_p), the diameter of spiral (D_s), the diameter of the spiral channel (d_r), and the spiral take-off angle (θ). These parameters are shown schematically in Fig. 1. The value of take-off angle (0) depends on the three other parameters mentioned above. In a constant spiral diameter, increasing the spiral pitch length will increase take-off angle. In a constant revolution diameter of 15 mm, changing the spiral pitch length creates different take-off angle. Spirals have take-off angle of 35°, 45°, 55° and 90° are investigated in this study.

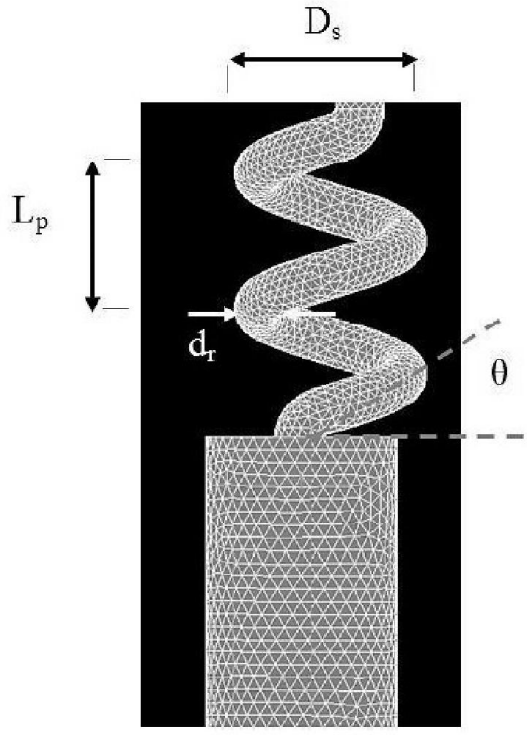

Fig. 1. Schematic illustration of a spiral crystal selector and design parameters

3. DIRECTIONAL SOLIDIFICATION

Four samples were produced from green wax rod having 5 mm diameter. They were made based on the designing parameters obtained from the simulation process. In all cases, the size of the starter block was 25 mm in diameter and 30 mm in the height. A cylindrical sample with diameter of 15 mm and the length of 50 mm was attached to the spiral part to study the final structure and the orientation of single crystal. The wax patterns were coated with alumina-zirconia refractory ceramic slurry several times to get a shell mold for casting.

The alloy used for experimental study was Al-3 wt. % Cu produced from pure aluminum (99.8 %) and copper (99.8%) in an electrical resistance furnace. Directional solidification experiments were carried out using a laboratory Bridgman type furnace. Pouring temperature of the melt was 800°C which was also applied in the simulation studies. After pouring the melt into the shell mold and holding it for a proper soaking time, the mold was withdrawn from the hot chamber at the rate of 3 mm. min^{-1}. Optical microscopy (OM, MEIJI TECHNO) was used to examine the structural features of the as solidified samples. To evaluate the crystallographic orientation of the single crystals, orientation map was acquired by electron back-scatter diffraction (EBSD) technique. To achieve this goal, the surface of the sample was electropolished to remove any strained surface and scratches. Oxford instrument EBSD detector was attached to Zeiss electron microscope for EBSD analysis. Aztech HKL software was used to index the pattern acquired for generating orientation maps and pole figure.

4. RESULTS AND DISCUSSION

The solidified structure of single crystal samples is shown in longitudinal cross section in Fig. 2. Except for the sample produced with take-off angle of 90° which is shown in Fig. 2d, all the other samples show single crystal structure with no high angle grain boundary among growing dendrites. The deviation of dendrites from <001> direction is depicted in this figure. As shown in

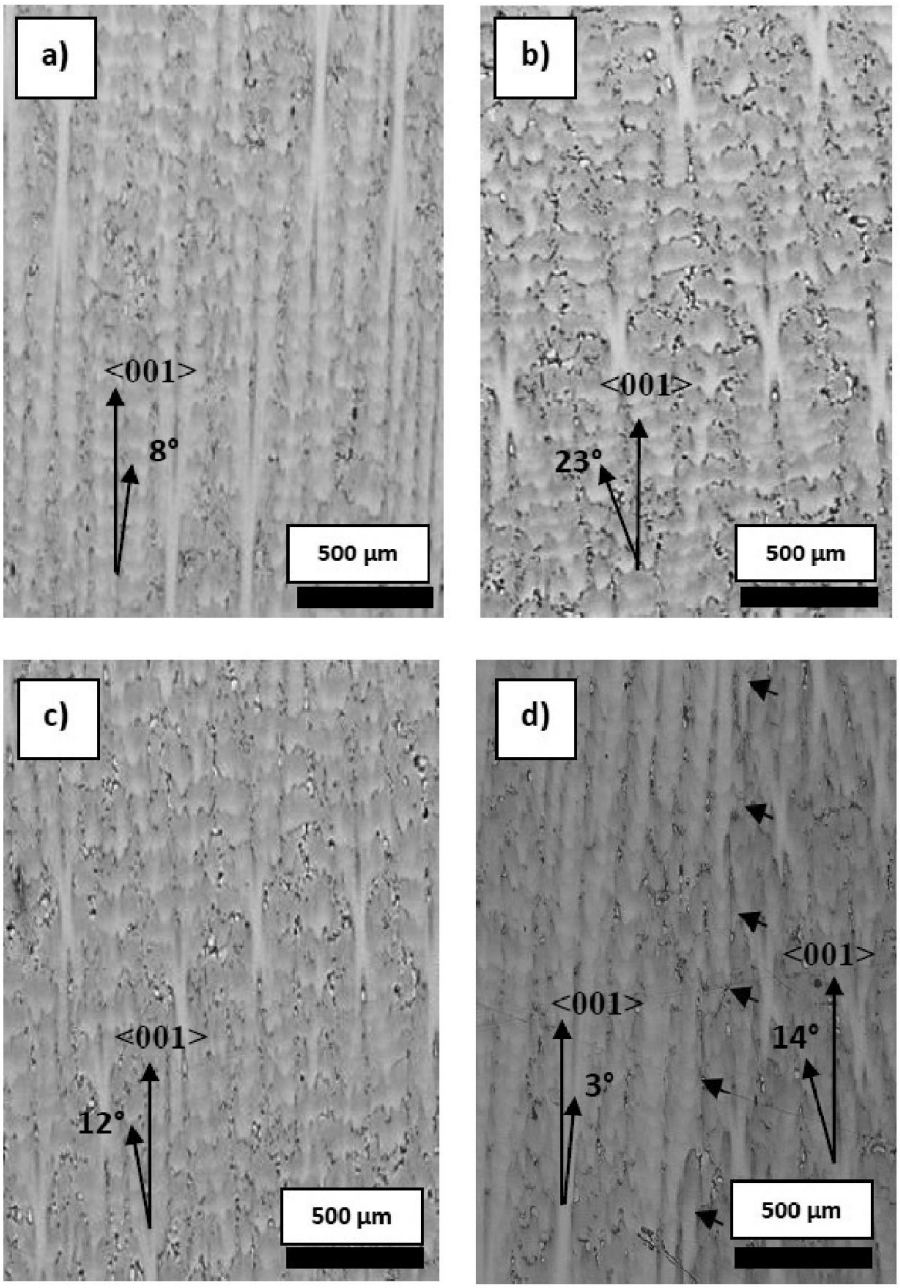

Fig. 2. Solidified structure of the alloys in longitudinal section and deviation of grains with respect to <001> direction for different take-off angle: a) 35° b) 45° c) 55° and d) 90°.

Fig. 2, for single crystal samples, by increasing the take-off angle of spiral crystal selector from 35° (Fig. 2a) to 45° (Fig. 2b), the deviation of crystal orientation increases from 8° to 23° from <001> direction. By further increase in take-off angle to 55°, the deviation of crystal orientation decreases to 12° from the preferred <001> direction (Fig. 2c). In the sample having take-off angle of 90°, a single grain is not obtained. The grain boundary between two neighboring grains is shown with black arrows. (Fig. 2d) The grain on the left hand side in Fig. 2d has the least deviation from <001> direction in comparison with the other single crystals shown in Fig. 2.

For the better understanding of the crystal orientation of the samples, corresponding <001>

pole figures of the directionally solidified samples are shown in Fig. 3. As shown in this figure, in all cases except than the sample with take-off angle equal to 90°, there exists just one grain in the final structure. There are 3 distinct grains in the sample with take-off angle of 90°. The deviation of the single grain from <001> direction for samples with take-off angle of 35° and 55° (Fig. 2a and 2b), is lower than that for the sample with take-off angle of 45° (Fig.2 c). For the samples with take-off angle of 35° and 55°, the deviation from <001> direction is less than 8° and 12°, respectively. There is about 23° deviation from <001> direction for the sample having take-off angle equal to 45°. While there is not a single grain in the sample having 90° take-off angle, there is a grain with the least misorientation (3°) in comparison with the other single crystals.

To investigate the effect of spiral shape on the crystal misorientation of the produced single grain, temperature distribution during solidification process has been studied using finite element calculations. Fig. 4 reveals the results obtained from finite element calculation in the domain after 1000 s and 4000 s. The solid fraction of solidified sample during time steps of the single crystal growth process is shown in this figure. As shown here, heat is extracted from the bottom of the sample and therefore, the solidification front moves upward. It creates a thermal gradient in the liquid and therefore, a mushy zone is formed in the solidification front.

The result obtained from CAFE calculations is shown in Fig. 5. As seen here, CAFE simulation predicts that by increasing the distance from the bottom of the sample, the number of grains will decrease in the starter block. This figure shows that, as solidification proceeds, the equiaxed

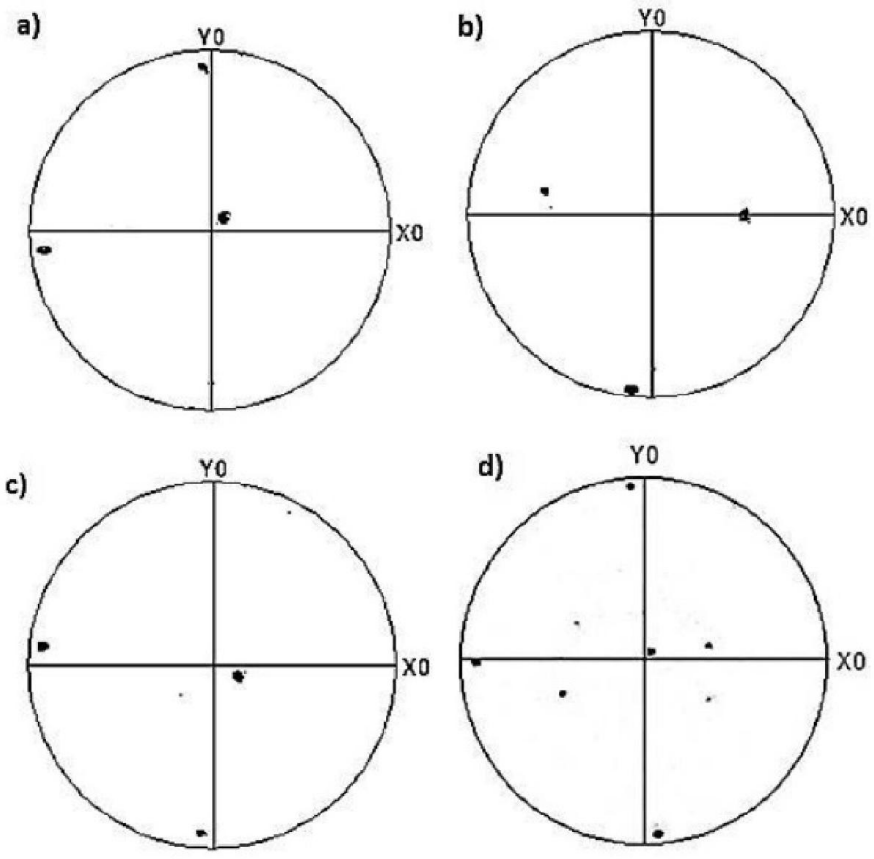

Fig. 3. <001> pole figure of samples for different spiral design: a) 35° b) 45° c) 55° and d) 90°.

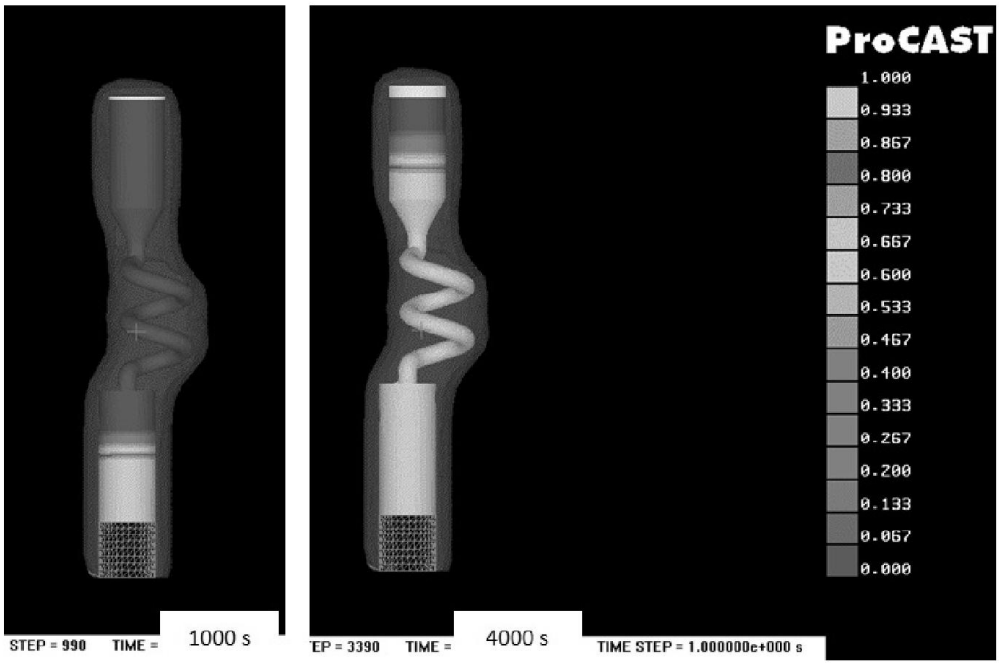

Fig. 4. variation of solid fraction after 1000 and 4000 s after the start of single crystal growth process.

crystal grains progressively evolve into parallel columnar grains with the competitive dendritic growth in starter block. The predicted pole figures revealed that the number of grains is decreased and they tend to <001> pole from point 1 to point 3 in the starter block. It is because of competitive growth of columnar grains which prefer to grow in the opposite direction of the heat flow direction. As shown in Fig. 5, at the point 3, the grains have deviation less than 20° from <001> direction. Also, there are few grains with deviation between 10° to 20°. Therefore, it can be concluded that a starter block with the height of 30 mm can be effective to create a well aligned <001> texture with deviation less than 20° from <001> direction.

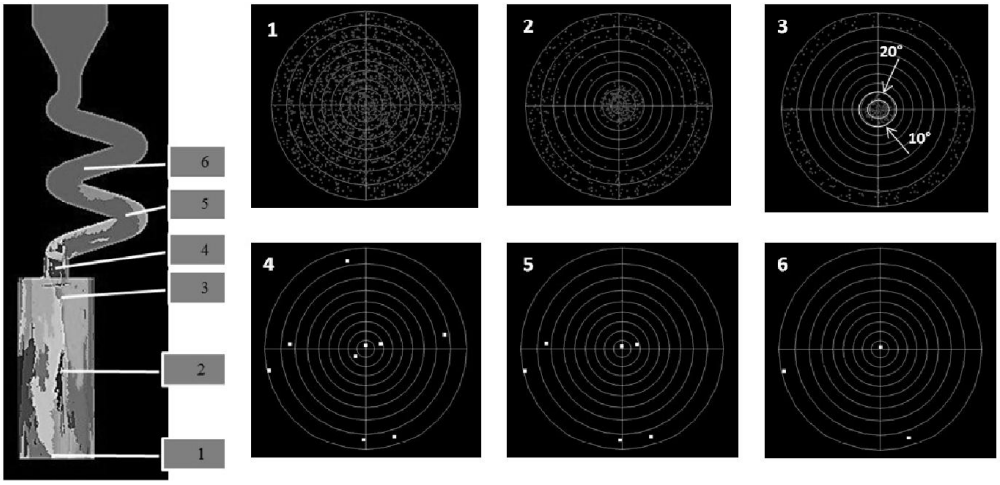

Fig. 5. simulated grain structure and the corresponding simulated pole figure of a solidified sample

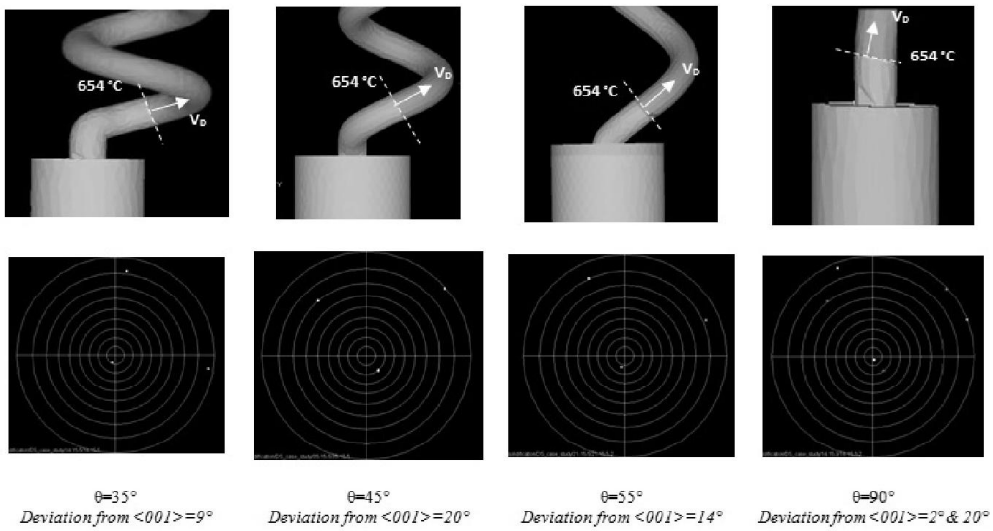

Fig. 6. Situation of liquidus isotherm (dashed line) at the spiral part for samples in this study and corresponding simulated pole figures.

When the solidification front reaches to the point 4 (at the entrance of the spiral channel) there are just three points remaining. At the point 5 (middle of the first revolution), one of the grains is blocked by the other grains and/or with the mold wall. Finally at the point 6, there is just a single grain. Heat flow direction at the entrance of the spiral part can affect the competitive growth between three grains remained at the entrance of the spiral channel. Simulation results revealed that the isotherm lines have been deviated where they enter the spiral channel. It is due to the effect of heat transfer from solidified portion of the sample which affects the heat flow direction. The magnitude of the deviation of isotherm line from the horizon mainly depends on the take-off angle of the spiral. As shown in Fig. 6, simulation results revealed that the direction of the normal vector of isotherm line varies with the variation of take-off angle. Increasing the take-off angle will increase the angle between the normal vectors of isotherm line from the horizon.

As indicated in Fig. 6, heat flow direction is the opposite of the normal vector (VD) of liquidus isotherm line which indicated as dashed line (654 °C). The corresponding simulated pole figure of the produced single crystal is also shown in Fig. 6. These results are in good agreement with the experimental results shown in Fig. 3. The results of experiments and simulation of the structure reveals that, increasing of the take-off angle from 35° to 45° will increase the misorientation of the single grain from <001> direction. But, further increasing of the take-off angle from 45 ° to 55° will decrease the misorientation from <001> again. For sample with the take-off angle equal to 90°, single grain is not obtained. But there exist a grain with misorientation less than 2° from <001> direction.

Where dendrites with random orientations arrive to the entrance of the spiral chanal, they begin to grow in the opposite of the heat flow direction. Dendrites having stems parallel or near the heat flow direction will grow easier. It is due to the growth anisotropy of cubic metals in which for cubic metals, <001> is known as preferred growth direction. So, dendrites tend to grow easier where their stem lay parallel to heat flow direction. As a result of competitive growth mechanism, dendrites with preferred growth direction parallel to the heat flow direction may over grown on non-preferred oriented grains and suppressed their further development [8]. In other word, based on competitive growth mechanism, dendrites which their stems are close to heat flow

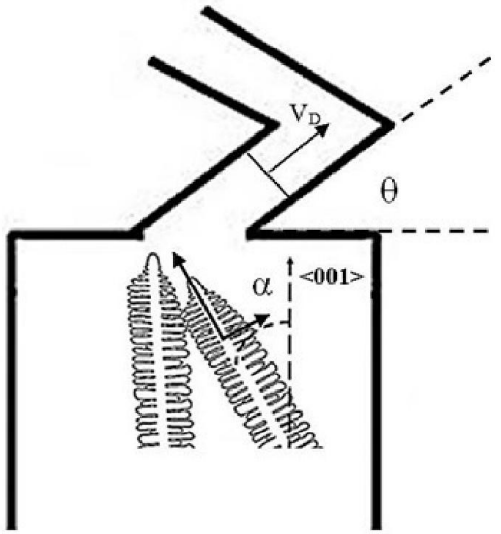

Fig. 7. Situation of growing dendrites against heat flow direction during entrance of spiral.

direction; have less growth undercooling and therefore, they can be consistent in growth process.

Selection of one grain in the spiral selector is carried out by blocking the primary dendrite arm and branching of secondary dendrite arms. As a result of four-fold symmetry of dendritic structure, secondary dendrite arms have also <001> direction. If the stem of dendrites or their secondary dendrites lay along normal vector, they will be in the preferred growth direction and will be consistent in competitive growth. As shown in Fig. 7, left-hand-side dendrite is growing along <001> direction and the dendrite in the right-hand-side is growing with a deviation equal to α from <001> direction. At the entrance of the spiral channel, secondary dendrite arms of the right-hand-side dendrite can grow easier. It is because that heat flow direction is along secondary dendrite arms of the mentioned dendrite. In this case, the undercooling for the growth of the secondary dendrite arm is less, and the dendrite will grow easier.

Based on the analytical model described above, it is concluded that when the spiral take-off angle tends to zero, secondary dendrite arms of well-oriented dendrite may grow easier. Therefore, decreasing the take-off angle can decrease the misorientation of the single crystal from <001> direction. On the other hand, where the take-off angle tends to vertical direction, dendrites with stems close to <001> direction will grow easier. But in this case, the role of spiral in the elimination of non-preferred oriented grains is weak. Therefore, a single grain may not be obtained in this situation. Based on the

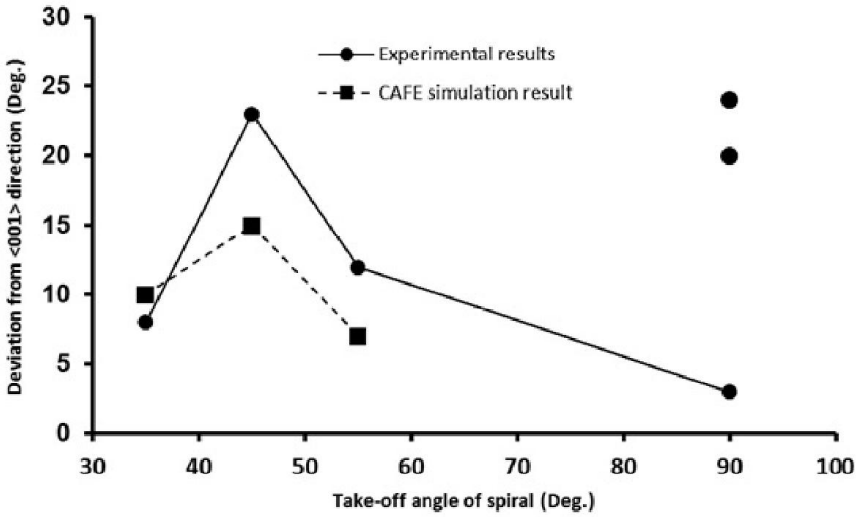

Fig. 8. Variation of crystal misorientation versus take-off angle of spiral crystal selector.

symmetry of dendritic structure as well as this fact that dendrite arms are perpendicular to each other, it can be concluded that the deviation of single crystal is between -45° to 45°. It is worth to note that, a well-designed starter block, produces a <001> texture having dendrites with deviation less than 10° to 20° to each other. It is reported that where the height of starter block is approximately 36 mm, the deviation of dendrites from <001> direction is less than 10° at the end of starter block. [16] In this study, the height of the starter block is set to 30 mm and experimental results revealed that the maximum deviation from <001> is about 20°. The experimental and CAFE numerical results obtained in this study have been compared in Fig. 8.

As shown in this figure, crystal deviation from <001> direction would be increased by increments of take-off angle of the spiral up to 45°. Further increase of take-off angle will decrease the deviation from preferred orientation. This phenomenon is mainly due to symmetry of dendrite structure.

There is more than one grain in the case of a vertical rod (90°) and therefore, three points are depicted for this sample in Fig. 8. Decreasing the take-off angle decreases the crystal deviation from preferred direction. But, single crystal structure may not be produced where take-off angle is less than 15°.

4. CONCLUSIONS

The effect of spiral crystal selector geometry on the grain orientation is evaluated using experimental and numerical simulation. The following conclusions can be summarized from this study:

1. A starter block with a height of 30 mm, yields a well aligned <001> texture with less than 20° deviation from <001> direction. Also, when the distance from the chill is increased in the starter block, the number of grains is decreased as a result of competitive growth mechanism.
2. Variation of spiral angle, will change the heat flow direction with respect to <001> direction. It is responsible for the grain misorientation in the spiral crystal selector. The dendrites at the entrance of the spiral passage which are aligned or lay close to the heat flow direction will be more consistent.
3. Increasing the spiral take-off angle from 35° up to 45°, increases the crystal misorientation from <001> direction. The misorientation of 8° and 23° from <001> direction is measured in the case of spirals with take-off angle of 35° and 45°, respectively. Increasing of take-off angle to 55° decreases the misorientation to 12° again. While increasing the spiral take-off angle greater than 45° reduces the misorientation from <001>, it will reduces the efficiency of spiral selector to select a single grain.

ACKNOWLEDGMENTS

The authors acknowledge the financial support of PARTO Company and MAPNA group in this project.

REFERENCES

1. Tin, S, Intelligent Alloy Design: Engineering Single Crystal Superalloys Amenable for Manufacture. Mater. Sci. Technol., 2009, 25, 136-146.
2. Wagner, A, Shollock, B. A, McLean M, Grain structure development in directional solidification of nickel-base superalloys, Mater. Sci. Eng. A, 2004, 374, 270-279
3. Rae, C. M. F, Zhang, L, Primary creep in single crystal superalloys: some comments on effects of composition and microstructure, Mater. Sci. Technol., 2009, 25, 228-235.
4. Das, N, Pandey, M. C, Ghosh, R. N, High temperature creep of a single crystal superalloy. Mater. Sci. Technol., 1998, 14, 429-434.
5. Xu, B. X, Wang, X. M, Zhao, B, Yue, Z. F, Study of crystallographic creep parameters of nickel-based single crystal superalloys by indentation method , Mater. Sci. Eng. A, 2008, 478,187–194.
6. Carter, P, Gandin, C. A, Reed, R. C, Process Modelling of Grain Selection during the Solidification of Single Crystal Superalloy

Castings, Mater. Sci. Eng. A, 2000, 280, 233–246.
7. Esaka, H, Shinozuka, K, Tamura, M, Analysis of single crystal casting process taking into account the shape of pigtail, Mater. Sci. Eng. A, 2005, 413-414, 151-155.
8. Toloraiya, V. N, Kablov, E. N, Advanced Method for Single Crystal Casting of Turbine Blades for Gas Turbine Engines and Plants, Metal Sci. Heat Treatment, 2002, 44, 279-284.
9. Zhou, Y. Z, Volek, A, Green, N. R, Mechanism of competitive grain growth in directional solidification of a nickel-base superalloy, Acta Mater., 2008, 56, 2631–2637.
10. Zhan, X. H, Dong, Z. B, Wei, Y. H, Ma, R, Simulation of grain morphologies and competitive growth in weld pool of Ni–Cr alloy, J. cryst. growth, 2009, 311, 4778-4783.
11. Li, J, Wang, Z, Wang, Y, Wang, J, Phase-field study of competitive dendritic growth of converging grains during directional solidification, Acta Mater., 2012, 60, 1478–1493.
12. D'Souza, N, Newell, M, Devendra, K, Jennings, P. A, Ardakani, M.G, Shollock, B. A, Formation of low angle boundaries in Ni-based superalloys, Mater. Sci. Eng. A, 2005, 413-414, 567–570.
13. Dai, H. J, Newell, M, Reed, R. C, D'Souza, N, Brown, P. D, Dong, H. B, Grain Selection during Solidification in Spiral Grain Selector, Superalloys, 2008, 367-374.
14. Wang, N, Liu, L, Gao, S, Zhao, X, Huang, T, Zhang, J, Fu, H, Simulation of grain selection during single crystal casting of a Ni-base superalloy, J. Alloys and Compounds, 2014, 586, 220 -229.
15. Meng, X, Lu, Q, Li, J, Jin, T, Sun, X, Zhang, J, Chen, Zh, Wang, Y, Hu, Zh, Modes of Grain Selection in Spiral Selector during Directional Solidification of Nickel-base Superalloys, J. Mater. Sci. Technol., 2012, 28, 214-220.
16. Dantzig, J. A., Rappaz, M, Solidification, EPFL press, Switzerland, 2008.
17. Dai, H. J, Dong, H. B, D'Souza, N, Gebelin, J. C., Reed, R. C., Grain selection in spiral selectors during investment casting of single-crystal turbine blades: part I. experimental investigation, Mater. Trans. A, 2011, 42, 3439-3446.
18. Dai, H. J, D'Souza, N, Dong, H. B, Grain selection in spiral selectors during investment casting of single-crystal components: part II. numerical modeling, Metall. Mater. Trans. A, 2011, 42, 3430-3438.
19. Gao, S. F, Liu, L, Wang, N, Zhao, X. B, Zhang, J, Fu, H. Z, Grain Selection During Casting Ni-Base, Single-Crystal Superalloys with Spiral Grain Selector, Metall. Mater. Trans. A, 2012, 43, 3767-3775.
20. Kurz, W, Giovanola, B, Trivedi, R, Theory of microstructural development during rapid solidification, Acta Metallurgica, 1986, 34, 823-830.